AIP | Journal of Applied Physics

Lattice thermal conductivity of ultra high temperature ceramics ZrB2 and HfB2 from atomistic simulations

John W. Lawson, Murray S. Daw, and Charles W. Bauschlicher

Citation: J. Appl. Phys. **110**, 083507 (2011); doi: 10.1063/1.3647754
View online: http://dx.doi.org/10.1063/1.3647754
View Table of Contents: http://jap.aip.org/resource/1/JAPIAU/v110/i8
Published by the American Institute of Physics.

Lattice thermal conductivity of ultra high temperature ceramics ZrB_2 and HfB_2 from atomistic simulations

John W. Lawson,[1,a)] Murray S. Daw,[2] and Charles W. Bauschlicher, Jr.[3]
[1]*Thermal Protection Materials Branch, Mail Stop 234-1, NASA Ames Research Center, Moffett Field, California 94035, USA*
[2]*Department of Physics and Astronomy, Clemson University, Clemson, South Carolina 29631, USA*
[3]*Entry Systems and Technology Division, Mail Stop 230-3, NASA Ames Research Center, Moffett Field, California 94035, USA*

(Received 24 June 2011; accepted 27 August 2011; published online 19 October 2011)

Atomistic Green-Kubo simulations are performed to evaluate the lattice thermal conductivity for single crystals of the ultra high temperature ceramics ZrB_2 and HfB_2. Recently developed interatomic potentials are used for these simulations. Heat current correlation functions show rapid oscillations, which can be identified with mixed metal-Boron optical phonon modes. Results for temperatures from 300K to 1000K are presented. © *2011 American Institute of Physics*. [doi:10.1063/1.3647754]

I. INTRODUCTION

The class of materials referred to as ultra high temperature ceramics (*UHTC*), including ZrB_2 and HfB_2, have high melting points, good chemical stability, and reasonable mechanical properties. They are candidate materials for applications involving high temperature environments, such as sharp leading edges for hypersonic vehicles, propulsion systems, and refractory crucibles.[1–3] They have also been discussed as buffer materials for microelectronics.[4] Unlike most ceramics, these materials are distinguished by their high thermal conductivity. High thermal conductivity offers a number of advantages for high temperature applications, including improved thermal shock resistance and enhanced thermal radiation by efficient distribution of thermal energy over available surfaces.

ZrB_2 and HfB_2 are broadly similar materials, but have nontrivial differences. *Zr* and *Hf* have comparable atomic radii and valence electronic structure, making their diboride analogues electronically almost indistinguishable. However, the large mass difference between *Zr* and *Hf* atoms leads to significant deviations, especially in the vibrational spectra of the diborides. These differences are expected to affect their lattice thermal conductivity as well. The crystal structure of ZrB_2 and HfB_2 is the AlB_2 -type *C*32 with space group *P6/mmm*. These materials are layered with alternating planes of close packed hexagonal *Zr/Hf* and open hexagonal, graphitic *B*. Metal atoms are situated directly above/below 6-membered rings in the adjacent Boron planes. A detailed *ab initio* study of the structure and properties of these materials was recently presented.[5]

High thermal conductivity ceramics, such as ZrB_2 and HfB_2, have significant contributions from both electronic and phononic thermal carriers to the total thermal conductivity κ_{tot}.[6] The electronic component κ_e can be estimated from the electrical conductivity σ using the Weidemann-Franz (WF) empirical relation, $\kappa_e = \kappa_0 \sigma T$, where κ_0 is the Lorentz constant ($2.45 \times 10^{-8} \mathrm{W} \cdot \Omega \cdot \mathrm{K}^{-2}$) and T is the temperature. The phonon part κ_{ph} cannot be measured directly and is usually inferred by subtracting κ_e from κ_{tot}. The lattice thermal conductivity can be accessed directly, however, from molecular dynamics (MD) simulations.

Thermal conductivity measurements for single crystal ZrB_2 at room temperature have been reported as $140\mathrm{W}/(\mathrm{m} \cdot \mathrm{K})$ in the basal direction and $100\mathrm{W}/(\mathrm{m} \cdot \mathrm{K})$ along the c-axis.[7] These single sample results included neither a characterization of defects that will reduce κ_{tot} nor individual estimates for κ_e and κ_{ph}. Thermal conductivity data has not been reported for single crystal HfB_2, although such samples have been fabricated.[8]

Thermal conductivity of polycrystalline ZrB_2 and HfB_2 has been more thoroughly studied.[9–12] Room temperature measurements give $60\mathrm{W}/(\mathrm{m} \cdot \mathrm{K})$ for ZrB_2 and $104\mathrm{W}/(\mathrm{m} \cdot \mathrm{K})$ for HfB_2. The reduction of κ_{tot} relative to single crystals comes primarily from the thermal resistance of grain boundaries. Variations of κ_{tot} with grain size can be substantial.[9,11] For ZrB_2 at 300K, κ_e was estimated to be $32\mathrm{W}/(\mathrm{m} \cdot \mathrm{K})$ using the WF relation, giving $28\mathrm{W}/(\mathrm{m} \cdot \mathrm{K})$ for κ_{ph}. As a function of temperature, κ_{tot} for polycrystalline ZrB_2 rises gradually up to at least 1800K, primarily due to a monotonically increasing κ_e. Conversely, κ_{ph} decreases as $1/T$, saturating to a value of $18\mathrm{W}/(\mathrm{m} \cdot \mathrm{K})$ above 1000K, which is well above the Debye temperature ($T_D = 750\mathrm{K}$) for this material. For HfB_2, κ_{tot} is generally higher than for ZrB_2, although a detailed comparison accounting for defect distributions and microstructure has not been done. Separate estimates for κ_{ph} in HfB_2 have not been made, although behavior similar to ZrB_2 is expected. Based on these results, we estimate the lattice contribution to κ_{tot} to be on the order of 40%. This suggests, for single crystals, that the lattice component will be at least $56\mathrm{W}/(\mathrm{m} \cdot \mathrm{K})$ within the planes and $40\mathrm{W}/(\mathrm{m} \cdot \mathrm{K})$ in the normal direction.

Recently, we developed Tersoff style interatomic potentials[13] for ZrB_2 and HfB_2. In this paper, we report results of atomistic Green-Kubo simulations of the lattice thermal conductivity κ_{ph} for single crystal ZrB_2 and HfB_2. Direct

a)Electronic mail: John.W.Lawson@nasa.gov.

measurement of κ_{ph} is difficult in materials with high κ_e; therefore, simulations of the lattice component can be useful to isolate that particular thermal conduction mechanism. These computations represent the first atomistic simulations for ZrB_2 and HfB_2 and also the first nontrivial test of these new potentials.

II. METHOD

The Green-Kubo (GK) theorem relates the lattice thermal conductivity tensor κ_{ij} to the integral of the ensemble average of the time correlation function of the heat current $J_i(t)$,

$$\kappa_{ij} = \frac{V}{k_B T^2} \int_0^\infty \langle J_i(0) J_j(t) \rangle dt, \tag{1}$$

where $i,j = x,y,z$, V is the volume, k_B is the Boltzmann's constant, and T is the temperature. The instantaneous heat current can be evaluated from the phase space configuration of the system at time t as

$$\vec{J}(t) = \frac{1}{V} \left[\sum_i e_i \vec{v}_i + \sum_{i<j} (\vec{f}_{ij} \cdot \vec{v}_j) \vec{x}_{ij} \right], \tag{2}$$

where e_i is the per atom energy of atom i, $\vec{f}_{ij}$ is the force on atom i due to neighbor j, $\vec{v}_i$ is the velocity of atom i, and $\vec{x}_{ij} = \vec{x}_i - \vec{x}_j$, where $\vec{x}_i$ is the position vector of atom i. The GK method implemented in the context of MD is essentially an exact method with the principal error dependent on the fidelity of the interatomic potentials. Solid argon, for example, which is well-described by a Lennard-Jones potential, gives thermal conductivity in very good agreement with experiment.[14]

MD simulations were performed using the LAMMPS package.[15] Systems were prepared first with a *NPT* run to allow the volume to expand, followed by a *NVE* run to equilibrate the system at the desired T. Timesteps ranging from 0.1 fs to 1 fs were used as required to maintain energy conservation. Larger timesteps were generally used at low T and smaller timesteps at higher T. After equilibration, time series data for the heat current was collected under *NVE*. To reduce statistical noise for κ, long *NVE* runs were required. For lower temperatures, $T = 300$K for example, runs of 10ns with a 1fs time step were performed. For higher temperatures with smaller timesteps, runs with a comparable or larger number of steps were used. The largest number of steps considered was 4×10^7 steps. Eight independent simulations were performed for each system and at each temperature to control for the randomized initial velocities.

Correlation functions were evaluated from the heat current time series. To increase the statistics, correlations were considered in a sliding window through the data set. This approach gives errors that increase with the correlation time. The integral of the heat current correlation function (*HCCF*) $C_{ij}(t) = \langle J_i(0) J_j(t) \rangle$ was evaluated using the trapezoid rule. Time correlations up to 200ps gave well-converged values for the thermal conductivity. A good discussion of the details of GK simulations can be found, for example, in Ref. 18.

Recently derived Tersoff style interatomic potentials[13] were used for both ZrB_2 and HfB_2. For ZrB_2, two potentials were developed that were denoted "Pot 1" and "Pot 2." "Pot 2," however, gives lattice thermal conductivity values for κ_{zz} that are higher than the in-plane component, which is not consistent with experiment. "Pot 1" does give the correct ordering, and therefore, we focus our investigations using it.

We consider defect-free, single crystals. Thus, the only scattering mechanism will be phonon-phonon scattering. Real materials, including single crystals, however, contain a non-trivial distribution of defects. Previous simulations have shown significant reductions in thermal conductivity, due to defect scattering.[16] Unit cells contained 12 atoms with 4 Zr/Hf atoms and 8 Boron atoms. Simulation cells of size $8 \times 8 \times 16$ were utilized, giving 12 288 atoms. Thermal conductivity values are well converged with respect to system size at this level.

III. RESULTS

Lattice thermal conductivity was obtained for both ZrB_2 and HfB_2 at temperatures of 300K, 600K, 800K, and 1000K. In Fig. 1, the normalized *HCCF* $C_{xx}(t)$ is presented for three different systems: ZrB_2 at $T = 300$K; HfB_2 at $T = 300$K; and HfB_2 at $T = 1000$K. Analogous results can be obtained for C_{yy} and C_{zz}. A distinctive feature of these curves is their rapid and regular oscillation. The oscillation frequency and decay for ZrB_2 and HfB_2 at 300K are similar, reflecting the broad commonalities of these materials. However, for HfB_2 at 1000K, there is significantly stronger damping. These features will be directly reflected in the values for κ. This oscillatory behavior is different from many *HCCFs* reported in the literature and is often seen in complex systems with a number of optical modes of similar frequency, for example, in silica.[17] The *HCCF* for monoatomic systems, such as silicon, may decay monotonically for long times, but can show oscillatory features for short times.[18] Oscillatory *HCCFs* have also been observed in systems with nontrivial mass differences.[19]

The *HCCF* oscillations can be analyzed in more detail by examining the Fourier transform. In Fig. 2, the power spectra for six different *HCCFs* are displayed: the C_{xx} and

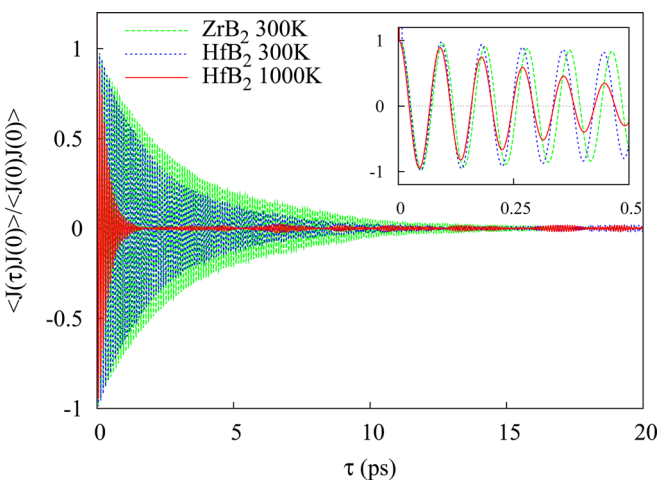

FIG. 1. (Color online) Normalized heat current correlation function (*HCCF*) for $C_{xx}(\tau)$ as a function of time. Unlike monoatomic systems, the *HCCF* for ZrB_2 and HfB_2 have rapid, regular oscillations.

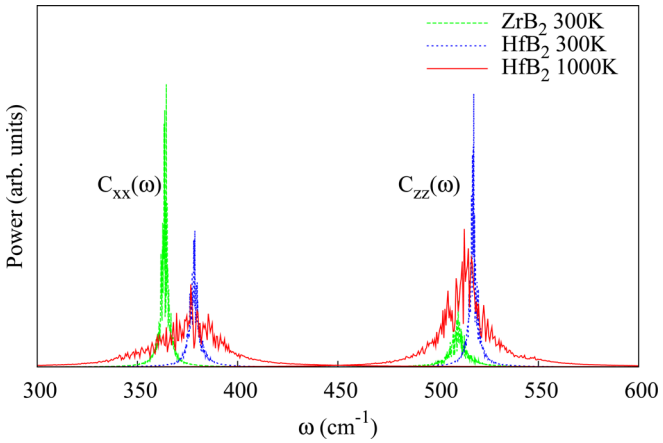

FIG. 2. (Color online) Power spectra of six heat current correlation functions obtained from Fourier transformation. Low temperature spectra are peaked around a single frequency identified with mixed metal-Boron optical phonon modes.

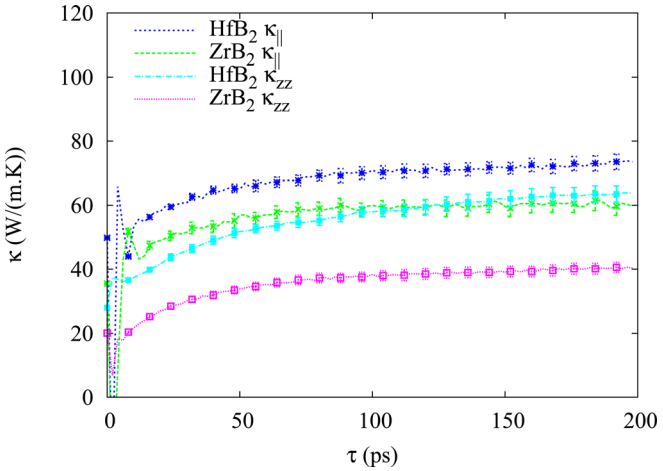

FIG. 3. (Color online) Integrated *HCCF* as a function of the upper integration limit τ, giving both in-plane (x-y plane) $\kappa_{||}$ and out-of-plane (z-direction) κ_{zz} conductivities at 300K for ZrB_2 and HfB_2.

C_{zz} components for ZrB_2 at $T = 300$K and the same components for HfB_2 at $T = 300$K and at $T = 1000$K. Interestingly, the spectra are peaked around single frequencies, which can be identified with specific optical phonon modes. Phonon spectra for these interatomic potentials have been calculated previously.[13] For example, for ZrB_2 at $T = 300$K, the power spectra for C_{xx} spikes at $\omega = 364\text{cm}^{-1}$. This frequency corresponds precisely to the in-plane $Zr - B$ optical phonon mode. Similarly, the C_{zz} spectra spikes at $\omega = 510\text{cm}^{-1}$, which matches the out-of-plane $Zr - B$ optical phonon mode. Analogous results are shown for HfB_2 at $T = 300$K. For HfB_2 at 1000K, we see a broadening of the peaks, due to anharmonic effects.

Numerical integration of the *HCCF* is shown in Fig. 3 for ZrB_2 and HfB_2 at $T = 300$K as a function of the upper integration limit τ. For each material, two independent components of the thermal conductivity tensor are shown: $\kappa_{||}$ is the average of the symmetric in-plane directions κ_{xx} and κ_{yy}; and κ_{zz} is normal to the planes. As can be seen, the curves plateau above 100ps, indicating largely converged integrals. Values for the ZrB_2 lattice thermal conductivity, when integrated out to 200ps, are $60\text{W}/(\text{m}\cdot\text{K})$ for the in-plane component and $41\text{W}/(\text{m}\cdot\text{K})$ in the normal direction. For HfB_2, the values are $74\text{W}/(\text{m}\cdot\text{K})$ and $63\text{W}/(\text{m}\cdot\text{K})$, respectively. For both of these materials, κ_{zz} is less than $\kappa_{||}$, which agrees with the experimental ordering. Values for HfB_2 are also higher than for ZrB_2.

Results for the *HCCF* are relatively free of statistical noise, which is a consequence of the very long runs we performed. Other methods have been reported in the literature to obtain reliable numbers from shorter runs. For example, fitting the *HCCF* to sums of exponentials has been proposed. However, the correct analytic form is not known at this time. Therefore, this approach could introduce errors. Modern computer power appears to be adequate to obtain sufficient statistical convergence without fitting.

Next, we consider the temperature dependence of the lattice thermal conductivity. In Fig. 4, we plot both the in-plane $\kappa_{||}$ and the normal κ_{zz} conductivities at four different temperatures: 300K, 600K, 800K, and 1000K for ZrB_2 and HfB_2. As expected, there is a rapid decrease as a function of T. In this temperature regime, anharmonic phonon scattering dominates with the phonon mean free path decreasing as $1/T$. Fits of the different data sets to $1/T$ are shown in the graph. All four curves converge to similar values for κ at high T, which at $T = 1000$K, is about $5\text{W}/(\text{m}\cdot\text{K})$. Compared to experiment, however, the high T values obtained from our simulations for κ are probably too low. Lattice thermal conductivity for polycrystalline ZrB_2, for example, saturates around $18\text{W}/(\text{m}\cdot\text{K})$, which can be considered a lower bound for our single crystal results. The low κ values at high T most likely reflect a limitation in the description of the anharmonic part of the interatomic potentials, which results in increased phonon-phonon scattering.

IV. DISCUSSION

Further insight can be obtained by considering the approximate relation $\bar{\kappa}_{ph} = \frac{1}{3}\rho C v_s \lambda_{ph}$, where ρ is the density, C is the specific heat, v_s is the velocity of sound, λ_{ph} is the phonon mean free path, and $\bar{\kappa}_{ph}$ is the isotropic lattice thermal

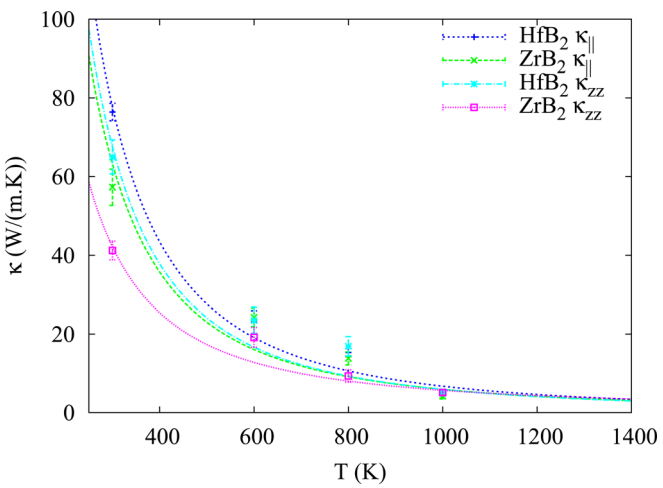

FIG. 4. (Color online) In-plane $\kappa_{||}$ and out-of-plane κ_{zz} lattice thermal conductivity as a function of temperature for ZrB_2 and HfB_2. Curves are fits of the data to $1/T$.

TABLE I. Room temperature properties for single crystal ZrB_2 and HfB_2, where ρ is the density, T_{melt} is the melting temperature, T_D is the Debye temperature, υ_s is the velocity of sound calculated from $\upsilon_s = 0.87\sqrt{E/\rho}$, where E is the bulk modulus, λ_{ph} is the phonon mean free path calculated from $\bar{\kappa}_{ph} = \frac{1}{3}\rho C \upsilon_s \lambda_{ph}$, and $\bar{\kappa}_{ph}$ is the isotropic lattice thermal conductivity.

		$\rho(\mathrm{g/cm^3})$	$T_{melt}(\mathrm{K})$	$T_D(\mathrm{K})$	$C(\mathrm{J/(mol\cdot K)})$	E (GPa)	$\upsilon_s(\mathrm{km/s})$	$\lambda_{ph}(\mathrm{nm})$	$\bar{\kappa}_{ph}(\mathrm{W/m\cdot K})$
ZrB_2	Exp.	6.119	3518	750	48.2	215	5.16	11.3	51
	MD					240	5.45	11.4	54
HfB_2	Exp.	11.212	3653	565	49.5	212	3.78	N/A	N/A
	MD					415	5.29	14.3	70

conductivity. Both experimental and computed values for these quantities are given in Table I. The specific heat of these materials is comparable with a value of $\sim 48\mathrm{J/(mol\cdot K)}$. The velocity of sound can be evaluated using $\upsilon_s = 0.87\sqrt{E/\rho}$, where E is the bulk modulus, giving 5.16km/s for ZrB_2 and 3.78km/s for HfB_2 based on the experimental values, while giving 5.45km/s for ZrB_2 and 5.29km/s for HfB_2 based on values from the interatomic potentials. Since $\upsilon_s \sim \sqrt{1/M}$, ZrB_2 is expected to have a higher υ_s than HfB_2, which is reflected in the υ_s derived from experimental numbers. However, the HfB_2 interatomic potential gives a modulus too high by a factor of 2X, thus the theoretical values of υ_s for the two materials are comparable. Estimates for the phonon mean free path can be obtained using experimental and simulation results for $\bar{\kappa}_{ph}$. For ZrB_2 at 300K, an experimental estimate of $51\mathrm{W/(m\cdot K)}$ for $\bar{\kappa}_{ph}$ gives $\lambda_{ph} = 11.3\mathrm{nm}$, while the simulation value of $54\mathrm{W/(m\cdot K)}$ for $\bar{\kappa}_{ph}$ gives $\lambda_{ph} = 11.4\mathrm{nm}$. These results are in very good agreement, although an accurate experimental estimate for $\bar{\kappa}_{ph}$ requires further study. For HfB_2 at 300K, experimental data is not available. The simulation value of $70\mathrm{W/(m\cdot K)}$ for $\bar{\kappa}_{ph}$ gives $\lambda_{ph} = 14.3\mathrm{nm}$ for that material.

V. CONCLUSIONS

In this paper, atomistic Green-Kubo simulations for the lattice thermal conductivity of ZrB_2 and HfB_2 were performed for a range of temperatures. Interatomic potentials for these materials were recently developed, and this paper represents the first non-trivial test of those potentials. Oscillations in the heat current correlation functions can be identified with mixed $Zr/Hf - B$ optical phonon modes arising from the large metal/Boron mass difference. Agreement with available experimental results is very good at room temperature, but is probably too low at higher temperatures, e.g., $T = 1000\mathrm{K}$.

ACKNOWLEDGMENTS

J.W.L. and C.W.B. are civil servants in the Entry Systems and Technology Division. M.S.D was supported under a NASA prime contract to ELORET Corporation. We benefited from discussions with Pawel Keblinski and Tapan Desai.

[1]M. J. Gasch, D. T. Ellerby, and S. M. Johnson, "Ultra high temperature ceramic composites," in *Handbook of Ceramic Composites*, edited by N. P. Bansal (Kluwer Academic, Boston, 2005), p. 197.
[2]W. G. Fahrenholtz, G. E. Hilmas, I. G. Talmy, and J. A. Zaykoski, J. Am. Ceram. Soc. **90**, 1347 (2007).
[3]S. M. Johnson, M. J. Gasch, T. H. Squire, J. W. Lawson, M. M. Stackpoole, and M. I. Gusman, *Proc. 7th International Conference on High Temperature Ceramic Matrix Composites (HT-CMC7)*, Bayreuth, Bavaria, Germany, 20-22 September 2010, p. 819.
[4]Y. Yamada-Takamura, Z. T. Wang, Y. Fujikawa, T. Sakurai, Q. K. Xue, J. Tolle, P.-L. Liu, A. V. G. Chizmeshya, J. Kouvetakis, and I. S. T. Tsong, Phys. Rev. Lett. **95**, 266105 (2005); T. N. Oder, P. Martin, J. Y. Lin, H. X. Jiang, J. R. Williams, and T. Isaacs-Smith, Appl. Phys. Lett. **88**, 183505 (2006).
[5]J. W. Lawson, C. W. Bauschicher, and M. S. Daw, "Ab initio calculations of the electronic, mechanical and thermal properties of ZrB_2 and HfB_2," J. Am. Ceram. Soc. **94**, 3494 (2011).
[6]W. S. Williams, JOM **49**, 38 (1997); W. S. Williams, JOM **50**, 62 (1998).
[7]H. Kinoshita, S. Otani, S. Kamiyama, H. Amano, I. Akasaki, J. Suda, and H. Matsunami, Jpn. J. Appl. Phys. **40**, L1280 (2001).
[8]W. Hayami, R. Souda, T. Aizawa, and T. Tanaka, Surf. Sci. **415**, 433 (1998).
[9]J. W. Zimmermann, G. E. Hilmas, W. G. Fahrenholtz, R. B. Dinwiddie, W. D. Porter, and H. Wang, J. Am. Ceram. Soc. **91**, 1405 (2008).
[10]M. J. Gasch, S. M. Johnson, and J. Marschall, J. Am. Ceram. Soc. **91**, 1423 (2008).
[11]L. Zhang, D. A. Pejakovic, J. Marschall, and M. Gasch, "Thermal and electrical transport properties of spark plasma-sintered HfB_2 and ZrB_2 ceramics," J. Am. Ceram. Soc. (in press).
[12]E. Wuchina, M. Opeka, S. Causey, K. Buesking, J. Spain, A. Cull, J. Routbort, and F. Guitierrez-Mora, J. Mater. Sci. **39**, 5939 (2004).
[13]M. S. Daw, J. W. Lawson, and C. W. Bauschicher, Comput. Mater. Sci. **50**, 2828 (2011).
[14]H. Kaburaki, J. Li, S. Yip, and H. Kimizuka, J. Appl. Phys. **102**, 043514 (2007).
[15]S. Plimpton, J. Comput. Phys. **117**, 1 (1995).
[16]J. Li, L. Porter, and S. Yip, J. Nucl. Mater. **255**, 139 (1998).
[17]A. J. H. McGaughey and M. Kaviany, Int. J. Heat Mass Transfer **47**, 1799 (2003).
[18]P. K. Schelling, S. R. Phillpot, and P. Keblinshki, Phys. Rev. B **65**, 144306 (2002).
[19]J. Che, T. Cagin, W. Deng, and W. A. Goddard, J. Phys. Chem. **113**, 6888 (2000).